Improved Prediction of Heats of Formation of Energetic Materials Using Quantum Mechanical Calculations

Edward F. C. Byrd* and Betsy M. Rice

U.S. Army Research Laboratory, Aberdeen Proving Ground, Maryland 21005-5069

Received: July 1, 2005; In Final Form: November 15, 2005

We present simple atom and group-equivalent methods that will convert quantum mechanical energies of molecules to gas phase heats of formation of CHNO systems. In addition, we predict heats of sublimation and vaporization derived from information obtained from the quantum-mechanically calculated electrostatic potential of each isolated molecule. The heats of sublimation and vaporization are combined with the aforementioned gas phase heats of formation to produce completely predicted condensed phase heats of formation. These semiempirical computational methods, calibrated using experimental information, were applied to a series of CHNO molecules for which no experimental information was used in the development of the methods. These methods improve upon an earlier effort of Rice et al. [Rice, B. M.; Pai, S. V.; Hare, J. *Combust. Flame* **1999**, *118*, 445] through the use of a larger basis set and the application of group equivalents. The root-mean-square deviation (rms) from experiment for the predicted group-equivalent gas phase heats of formation is 3.2 kcal/mol with a maximum deviation of 6.5 kcal/mol. The rms and maximum deviation of the predicted liquid heats of formation are 3.2 and 7.4 kcal/mol, respectively. Finally, the rms and maximum deviation of predicted solid heats of formation are 5.6 and 12.2 kcal/mol, respectively, an improvement in the rms of approximately 40% compared to the earlier Rice et al. predictions using atom equivalents and a smaller basis set (B3LYP/6-31G*).

1. Introduction

In an effort to make the best use of limited resources and to minimize the waste ensuing from experimental measurements, computational methods have been developed to aid in the formulation of advanced propellants and explosives.[1] The screening of hypothetical energetic materials through computational modeling allows experimental researchers to expend resources only on those molecules that show promise of enhanced performance, reduced sensitivity, or reduced environmental hazard.

A key property of an energetic material that is used to assess its potential performance in a gun or warhead is its heat of formation ($\Delta H°_f$). For notional compounds, significant resources could be expended in synthesizing the material, only to discover upon measuring its $\Delta H°_f$ that it is an unsuitable candidate for use. Therefore, efforts have been made to develop computational tools that will predict this important property a priori.[2−10] This paper presents a refinement of the computational tools developed by Rice et al.[10] that utilize quantum mechanical calculations to predict the heats of formation of energetic materials in the solid, liquid, and vapor phases.

There are several methods that predict gas phase heats of formation ($\Delta H°_{f(g)}$) from quantum mechanical calculations.[10−14] Theories using high-level treatment of electron correlation, such as the G2/G3 (and assorted hybrids) schemes,[11−12] are usually highly accurate but suffer from the scaling problems normally encountered by such theories when applied to large molecules. Other methods, such as those based on Hess's law,[14] usually require reliable experimental heats of formation for all components of the reaction except for the one being predicted, and an accurate heat of reaction. The availability of such thermodynamic data is often very limited, particularly with regard to some of the emerging exotic energetic materials.

For these reasons, Rice, Pai, and Hare developed a semiempirical atom-equivalent tool based on density functional theory[15,16] (DFT) calculations that predicted gas phase heats of formation of CHNO molecules.[10] This procedure was chosen because it produced fairly accurate results with only modest computational requirements. The atom equivalent gas-phase heat of formation for a particular molecule is written as

$$\Delta H°_{f(g)} = E - \sum n_j \epsilon_j \qquad (1)$$

where E is the quantum mechanically determined electronic energy of the molecule, n_j is the number of atom type j contained in the molecule, and ϵ_j is the "atom equivalent" energy of atom j. The ϵ_j are determined through a least-squares fit of eq 1 to a series of E and experimentally reliable $\Delta H°_{f(g)}$ values for a set of "training" molecules. As this method is semiempirical, care must be taken to ensure that the training set contains representative atom types in compounds for which the tool is parametrized. Thus, the tool is limited to prediction of the $\Delta H°_{f(g)}$ for the representative compounds. For example, attempting to predict the $\Delta H°_{f(g)}$ of a sulfur-containing compound would result in a failure of the method, as no molecules containing sulfur were used in parametrizing the tool. Representative compounds of conventional CHNO energetic materials include molecules with the nitro, nitroso, or azido functional groups. Molecules in this study include nitroaliphatics, nitroaromatics, nitramines, and nitrate esters, azidoaliphatics, and azidoaromatics. While limited in predictive capability, the atom-equivalent method offers the advantages of not requiring high-correlation quantum mechanical theories or needing additional experimental values after the initial fit has been completed.

10.1021/jp0536192
Published on Web 12/23/2005

Rice et al.[10] calculated the optimized structures and corresponding energies for 35 molecules containing functional groups common to CHNO explosives at the B3LPY/6-31G* level. They determined the atom equivalents through a least-squares fitting of eq 1 using these energies and experimental gas-phase heats of formation. As a means to encompass the different types of functional groups (i.e. for oxygen −CHO versus −COH), seven different atom types were defined: those atom types with single Lewis structures and those with multiple Lewis structures. The seven atom types are divided into four representing single-bonded atoms, namely, C, H, N, and O, while the remaining three are those atoms that are involved in multiple-bonded environments, namely, C′, N′, and O′. The root-mean-square (rms) deviation of the predicted $\Delta H°_{f(g)}$ from experiment was 3.1 kcal/mol, with a maximum deviation of 7.3 kcal/mol.[10]

For assessment of the potential performance of the energetic material of interest, however, the desired quantity is usually the condensed phase $\Delta H°_f$. To accommodate this need, Rice et al. applied a procedure proposed by Politzer and co-workers[17−19] to calculate the solid and liquid phase heats of formation using predicted heats of vaporization (ΔH_{vap}) and heats of sublimation (ΔH_{sub}). According to Hess's law,[14] the solid phase heat of formation ($\Delta H°_{f(s)}$) can be obtained by

$$\Delta H°_{f(s)} = \Delta H°_{f(g)} - \Delta H_{sub} \quad (2)$$

with a similar equation for the liquid phase heat of formation ($\Delta H°_{f(l)}$) using the heat of vaporization instead of ΔH_{sub}. Politzer et al.[17−19] demonstrated that correlations could be established between statistically based quantities of electrostatic potentials (ESP) mapped onto isodensity surfaces of isolated molecules and their heats of sublimation and vaporization. The predicted heat of vaporization can be represented as

$$\Delta H_{vap} = a\sqrt{(SA)} + b\sqrt{(\sigma^2_{tot}\nu)} + c \quad (3)$$

where SA is the surface area of the 0.001 electron/bohr^3 isosurface of the electron density of the molecule, σ^2_{tot} is a measure of the variability of electronic potential on the surface, and ν is the degree of balance between the positive and negative charges on the isosurface. The latter two quantities have been shown by Politzer et al. to be important in treating macroscopic properties that are dependent on noncovalent electrostatic interactions.[17−19] The constants *a*, *b*, and *c* are determined through a least-squares fit of eq 3 with experimental values for ΔH_{vap}. Similarly, the equation for the prediction of the heat of sublimation is written as

$$\Delta H_{sub} = a(SA)^2 + b\sqrt{(\sigma^2_{tot}\nu)} + c \quad (4)$$

with a different set of fitted *a*, *b*, and *c* parameters. This method of predicting the heats of vaporization or sublimation will be referred to hereafter as the "ESP method".

While the method prescribed in Rice et al.[10] has demonstrated its utility, the error in the $\Delta H°_{f\ (s)}$ predictions was larger than most propellant and explosive formulators prefer (2 kcal/mol).[20]

For example, the rms and maximum deviations of predicted solid phase heats of formation from 75 measured values were 9.0 and 35.0 kcal/mol, respectively. The causes for the errors could be due to a variety of reasons. First, some of the error could be attributed to varying and conflicting experimental information. For instance, numerous systems reported in ref 2 had different measured values of the heats of formation, sublimation, or vaporization. Second, it is possible that the simple application of the method of atom equivalents did not adequately represent the gas phase heats of formation for the variety of different classes of CHNO explosives. Third, a modest level of quantum mechanical theory (B3LYP/6-31G*) was used due to computational restrictions and sizes of the molecules studied. Fourth, the tool was parametrized from a set of experimental information assumed to adequately represent all of the various classes of CHNO explosives. Unfortunately, there is a limited amount of such measured data. Finally, many of the experimental molecular structures in the condensed phase were not used as initial starting points for the geometry optimizations due to limited knowledge. Subsequently, conformers used in the calculations might not necessarily correspond to experimental counterparts in the crystalline or liquid phases. This study is undertaken to eliminate these sources of error where possible, and determine if our efforts will provide a more accurate means of predicting the heats of formation of CHNO energetic materials.

2. Experimental Data Used in the Study

Two sets of data are discussed throughout this paper: The first is denoted as the training set, and it contains information about CHNO systems that are used in parametrizing eqs 1, 3, and 4. The second is denoted as the test set, which contains information that is used to assess the accuracy of the computational tools developed by fitting to information from the training suite. Experimental thermodynamic information for these compounds is given in Table 1S (Supporting Information).

Because the procedure requires using optimized geometries, the results could be dependent upon the initial molecular structures used in the geometry optimizations. For the training set, we had hoped to include only those molecules that had both experimental crystal structures that could be used as initial states in the geometry optimizations and a measured heat of vaporization or heat of sublimation. We also wanted systems that are representative of various classes of CHNO explosives. However, limited heat of vaporization data and information on compounds containing azido functional groups ($-N_3$) forced us to relax our original requirements for inclusion in the training set. The following molecules were added to the training set, regardless of their lack of experimental crystal structural information: 2-hydroxymethyl-2-methyl-1,3-propanediol trinitrate azidobenzene, azidomethylbenzene, 1-azido-1,1-dinitroethane, 1-azidoadamantane, 2-azido-2-phenylpropane, azidotrinitromethane, 3-azido-3-ethylpentane, and tetranitromethane. In order to expand our fitting suite of gas-phase training molecules, we also included *N*-nitrobis-2,2,2-trinitroethylamine, HNS (1,1′-(1,2-ethenediyl)bis[2,4,6−trinitrobenzene]), and *N*-nitrobis-2,2-dinitropropylamine as they possessed experimental structures but only gas phase heats of formation (no heats of vaporization or sublimation). Finally, we included TTT (hexahydro-1,3,5-trinitroso-1,3,5-triazine) to increase the number of nitroso functional groups (−NO), even though we could not find experimental structural data. The total number of molecules in the training set is 38 (Table 1), with 30 molecules having measured $\Delta H°_{f(g)}$, 23 having measured ΔH_{sub} values, and 10 molecules having measured ΔH_{vap} information. The set consists of nitroaliphatic, nitroaromatic, nitramine, and azido-containing compounds. Additionally, two of the systems contain the *N*-nitroso functionality.

One of the major concerns in any parametrization is the quality of data used in the fitting. Many of the molecules included in this study had multiple different experimental values for the various thermodynamic properties of interest. In the interest of a consistent algorithm and as not to bias the fitted

TABLE 1: List of Molecules[a] Included in Fitting Set (38 Molecules)

name	expt[b,c]	formula
nitromethane	g, l, v	CH_3NO_2
trinitromethane	l, s, v, sub	CHN_3O_6
tetranitromethane	g, l, v	*CN_4O_8*
azidotrinitromethane	g, l, v[d]	*CN_6O_6*
DMNO (*N*-methyl-*N*-nitromethanamine)	g, l, s, sub	$C_2H_6N_2O_2$
1-azido-1,1-dinitroethane	g, l, v[d]	*$C_2H_3N_5O_4$*
hexanitroethane	g, s, sub	$C_2N_6O_{12}$
nitroglycerin	g, l, v	$C_3H_5N_3O_9$
TTT (hexahydro-1,3,5-trinitroso-1,3,5-triazine)	g, s, sub	*$C_3H_6N_6O_3$*
RDX (cyclotrimethylene-trinitramine)	g, s, sub	$C_3H_6N_6O_6$
1,4-dinitrosopiperazine	g, s, sub	$C_4H_8N_4O_2$
1,4-dinitropiperazine	g, s, sub	$C_4H_8N_4O_4$
N-nitrobis-2,2,2-trinitroethylamine	g, s	$C_4H_4N_8O_{14}$
2-hydroxymethyl-2-methyl-1,3-propanediol trinitrate	s, v	*$C_5H_9N_3O_9$*
PETN (pentaerythritol tetranitrate)	s, sub	$C_5H_8N_4O_{12}$
nitrobenzene	g, l, v	$C_6H_5NO_2$
2-nitrophenol	g, s, sub	$C_6H_5NO_3$
3-nitrophenol	g, s, sub	$C_6H_5NO_3$
4-nitrophenol	g, s, sub	$C_6H_5NO_3$
m-nitroaniline	g, s, sub	$C_6H_6N_2O_2$
o-nitroaniline	s, sub	$C_6H_6N_2O_2$
p-nitroaniline	g, s, sub	$C_6H_6N_2O_2$
1,3-dinitrobenzene	l, s, sub	$C_6H_4N_2O_4$
azidobenzene	g, l, v	*$C_6H_5N_3$*
TNB (1,3,5-trinitrobenzene)	s, sub	$C_6H_3N_3O_6$
1-azido-4-nitrobenzene	g, s, sub	$C_6H_4N_4O_2$
N-nitrobis-2,2-dinitropropylamine (DNPN)	g, s	$C_6H_{10}N_6O_{10}$
PNT (1-methyl-4-nitrobenzene)	g, s, sub	$C_7H_7NO_2$
2,4-DNT (1-methyl-2,4-dinitrobenzene)	g, s, sub	$C_7H_6N_2O_4$
azidomethylbenzene	g, l, v	*$C_7H_7N_3$*
3-azido-3-ethylpentane	g[e]	*$C_7H_{15}N_3$*
TNT (trinitrotoluene)	g, s, sub	$C_7H_5N_3O_6$
2-ethoxy-1,3,5-trinitrobenzene	sub	$C_8H_7N_3O_7$
2,2-dinitroadamantane	g, s, sub	$C_{10}H_{14}N_2O_4$
1-azidoadamantane	g[e]	*$C_{10}H_{15}N_3$*
2-azido-2-phenylpropane	g[e]	*$C_{10}H_{13}N_3$*
HNS (1,1′-(1,2-ethenediyl)bis[2,4,6-trinitrobenzene])	g, s	$C_{14}H_6N_6O_{12}$
trityl azide	s, sub	$C_{19}H_{15}N_3$

[a] Molecules in italics did not have an experimental crystal structure from which to start. [b] Symbols denote what type of experimental data are available for each species: gas-phase heat of formation (g), liquid-phase heat of formation (l), solid-phase heat of formation (s), heat of sublimation (sub), and heat of vaporization (v). [c] References 21, 22. [d] Reference 23. [e] Reference 24.

parameters toward molecules that had more than one experimental datum to use in the parametrization, we arbitrarily chose to employ the most recently published value unless it was clear that the experimental information was poor. Likewise, when comparing predicted values with those in the test suite of molecules, we used the most recently published experimental data point.

The test set, listed in Table 2, includes molecules for which experimental structural data are missing or molecules for which experimental structures are known, but which lack thermodynamic data with which to fit. For several of the molecules lacking experimental structural data we performed a limited conformer search by starting at different initial geometries and allowing each to relax to a local energy minimum as prescribed by the B3LYP/6-31G* [27−29] forces. Like the training set, the test set is composed of nitroaliphatic, nitroaromatic, nitramine, and azido-containing compounds. However, it also contains compounds with chemical functionalities not included in the training set: nitrites, nitrotriazoles, nitrofuroxans, and C-nitroso species.

3. Computational Details

Geometry optimizations, electronic energy computations, and generation of electrostatic potentials of all molecules in the training and test sets were done utilizing the Gaussian 03 (G03) quantum mechanical program package.[30] The B3LYP hybrid generalized-gradient approximation (GGA) density functional theory (DFT)[27,28] was used with the 6-31G* basis set[29] to optimize geometries. Normal-mode analyses were performed for all systems containing no more than 21 heavy atoms to confirm that the optimized structure corresponded to a local minimum on the potential energy surface. For molecules with more than 21 heavy atoms, the optimized structure is assumed to correspond to a local potential energy minimum. The 6-311++G(2df,2p) basis set[31,32] was used to determine the densities for generating the electrostatic potentials (ESPs) and in determining the atom and group equivalents. Molecular properties used in eqs 1, 3, and 4 generated from the quantum mechanical calculations are provided in Table 2S (Supporting Information).

We also evaluated the effect on the predictive capability of the tools when using structures optimized using a larger basis set. We optimized the geometries using the 6-311++G(2df,-2p) basis set for a majority of the molecules included in this study, and reparametrized the computational tools. The resulting predictions were not in appreciably better agreement with experiment than those produced using methods associated with the B3LYP/6-31G* optimized structures. Since the effect was negligible, all calculations reported herein use B3LYP/6-31G* optimized structures. All geometries were allowed to relax to default G03 settings, with the energy converged to 10^{-8} hartrees.

In addition to generating atom equivalents for eq 1 from the B3LYP/6-311++G(2df,2p)//6-31G* energies, we used a group-equivalent scheme similar to the atom-equivalent scheme, where the gas phase heat of formation as represented in eq 1 now defines ϵ_j as the "group equivalent" energy and n_j refers to the number of group type j within the molecule instead of atom type. The groups that were included represent nitro groups attached to carbon (nitroaliphatics or nitroaromatic), nitrogen (nitramine), or oxygen (nitrate esters). Additionally, we have included a group representing the azide functionalities bonded to carbon atoms only. For those atoms within a molecule that do not belong to one of the specified groups (e.g. H, the oxygen in a carbonyl group) atom equivalent energies are used in eq 1. To accommodate this requirement for atoms not belonging to a specified group, new atom equivalent energies are generated in conjunction with the group equivalent energies. For both the atom and group equivalent schemes, the atom and group equivalents determined by eq 1 are correlated to experimental heats of formation for several representative molecules.

An alternate method for predicting the heat of sublimation of these materials was also evaluated. This approach, referred to as the quantitative structure property relationship (QSPR) method,[33,34] is used to establish relations between molecular structures with their chemical or physical properties. The QSPR approach using the CODESSA suite of QSPR software[35] was applied to the training set of molecules. Various combinations of available molecular descriptors were used to establish correlations with the heats of sublimation with the restriction that each combination could contain only five descriptors. The final set that was chosen for this exercise is the one that provided the largest R^2 value (0.9814) and cross-validated (CV) R^2 value (0.9662).[35] These five descriptors, described in the CODESSA User's manual,[35] are the WNSA-3 weighted PNSA (PNSA3*TMSA/1000) [Quantum-Chemical PC], PPSA-3 atomic charge weighted PPSA [Zefirov's PC], RNCG relative negative charge (QMNEG/QTMINUS) [Zefirov's PC], principal moment of inertia *C*/number of atoms, and the Kier and Hall index (order

TABLE 2: List of Molecules[a] Included in Test Set

name	expt[b,c]	formula	name	expt[b,c]	formula
methyl nitrite	g, l, v	CH_3NO_2	1,4-dinitrobenzene	s	$C_6H_4N_2O_4$
methyl nitrate	g, v	CH_3NO_3	triclinic 2,3-dimethyl-2,3-dinitrobutane	s	$C_6H_{12}N_2O_4$
dinitromethane	g, l, v	$CH_2N_2O_4$	α-DNP (2,4-dinitrophenol)	s	$C_6H_4N_2O_5$
nitroguanidine	s	$CH_4N_4O_2$	*β*-DNP (2,6-dinitrophenol)	s	$C_6H_4N_2O_5$
nitroguanyl azide	s	$CH_2N_6O_2$	4,6-dinitro-1,3-benzenediol	s	$C_6H_4N_2O_6$
ethyl nitrite	g	$C_2H_5NO_2$	*azidocyclohexane*[e]	l, v	$C_6H_{11}N_3$
nitroethane	l, v	$C_2H_5NO_2$	*1-azidohexane*	l, v	$C_6H_{13}N_3$
ethyl nitrate	g, l, v	$C_2H_5NO_3$	2,4,6-trinitrophenol	s	$C_6H_3N_3O_7$
2,2,2-trinitroethanol	s	$C_2H_3N_3O_7$	*2,4,6-trinitroresorcinol*	s	$C_6H_3N_3O_8$
5-nitro-*s*-triazol-3-ol	s	$C_2H_2N_4O_3$	*ETTN (2-ethyl-2-hydroxymethyl-1,3-propanediol trinitrate)*	s	$C_6H_{11}N_3O_9$
FOX-7 (1,1-diamino-2,2-dinitroethylene)	s[d]	$C_2H_4N_4O_4$	2,4-DNPH (2,4-dinitrophenyl hydrazine)	s	$C_6H_6N_4O_4$
N,N′-dinitro-1,2-ethanediamine	s	$C_2H_6N_4O_4$	NFS (5-nitro furfural semicarbazone)	s	$C_6H_6N_4O_4$
1-nitro-3-guanidinourea[e]	s	$C_2H_5N_5O_3$	2,4,6-trinitrobenzenamine (2,4,6-trinitroaniline)	s	$C_6H_4N_4O_6$
5,5′-hydrazotetrazole[e]	s	$C_2H_4N_{10}$	*DATB (2,4,6-trinitro-1,3-benzenediamine)*	s	$C_6H_5N_5O_6$
1-nitropropane	l, v	$C_3H_7NO_2$	TNA (2,3,4,6-tetranitro-aniline)	s	$C_6H_3N_5O_8$
2-nitropropane	l, v	$C_3H_7NO_2$	benzotrifuroxan	s	$C_6N_6O_6$
propyl nitrite	g, l, v	$C_3H_7NO_2$	TATB (2,4,6-trinitro-1,3,5-benzenetriamine)	s	$C_6H_6N_6O_6$
propyl nitrate	l, v	$C_3H_7NO_3$	*N,N′-dinitro-N,N′-bis(2-hydroxyethyl)-oxamidedinatrate*	s	$C_6H_8N_6O_{12}$
3-methyl-4-nitrofuroxan	s	$C_3H_3N_3O_4$	*4,4,4-trinitrobutyric acid 2,2,2-trinitroethyl ester*	s	$C_6H_6N_6O_{14}$
2-(methylnitroamino)ethanol nitrate	s	$C_3H_7N_3O_5$	*hexanitrol*	s	$C_6H_8N_6O_{18}$
1-nitrobutane	l, v	$C_4H_9NO_2$	*ϵ*-CL20 (*ϵ*-hexanitrohexa-azaisowurtzitane)	s[f]	$C_6H_6N_{12}O_{12}$
2-nitrobutane	l, v	$C_4H_9NO_2$	*nitromethylbenzene*	g, l, v	$C_7H_7NO_2$
2-methyl-2-nitropropane (tert-butyl nitrate)	g, s	$C_4H_9NO_2$	2,6-DNT (2-methyl-1,3-dinitrobenzene)	s	$C_7H_6N_2O_4$
n-butyl nitrite	g, l, v	$C_4H_9NO_2$	*dinitromethylbenzene*	g, s, sub	$C_7H_6N_2O_4$
tert-butyl nitrite	g, l, v	$C_4H_9NO_2$	*2-methyl-4,6-dinitrophenol*	s	$C_7H_6N_2O_5$
N-ethyl-N-nitroethanamine	l	$C_4H_{10}N_2O_2$	*1-azidoheptane*	l, v	$C_7H_{15}N_3$
butane-1,2,4-triyl nitrate	l	$C_4H_7N_3O_9$	*2-methoxy-1,3,5-trinitrobenzene*	s, sub	$C_7H_5N_3O_7$
3,4-furazandimethanol dinitrate	g, l, v	$C_4H_4N_4O_7$	2,4,6-trinitrobenzoic acid	s	$C_7H_3N_3O_8$
2,2,3,3-tetranitrobutane	s	$C_4H_6N_4O_8$	methylglucoside tetranitrate	s	$C_7H_{10}N_4O_{14}$
monoclinic 2,2′-nitroiminodiethanol (Dina)	l, s	$C_4H_8N_4O_8$	tetryl (*N*-methyl-*N*,2,4,6-tetranitroaniline)	s	$C_7H_5N_5O_8$
β-HMX (1,3,5,7-tetranitro-1,3,5,7-tetra-azacyclo-octane)	s	$C_4H_8N_8O_8$	*1,3-dimethyl-2-nitrobenzene*	g, l, v	$C_8H_9NO_2$
1-nitropiperidine	g, l	$C_5H_{10}N_2O_2$	*1-azidooctane*	l, v	$C_8H_{17}N_3$
azidocyclopentane[e]	l, v	$C_5H_9N_3$	TNX (2,4,6-trinitromethaxylene)	s	$C_8H_7N_3O_6$
1-azidopentane	l	$C_5H_{11}N_3$	1,3,5-trimethyl-2,4,6-trinitrobenzene	s	$C_9H_9N_3O_6$
DPT (dinitropentamethylenetetramine)[e]	s	$C_5H_{10}N_6O_4$	*1-nitronaphthalene*	s, sub	$C_{10}H_7NO_2$
1,1,1,3,5,5,5-heptanitropentane	s	$C_5H_5N_7O_{14}$	1,8-dinitronaphthalene	s	$C_{10}H_6N_2O_4$
nitrosobenzene	g, sub	C_6H_5NO	*dipentaerythritol hexanitrae*	s	$C_{10}H_{16}N_6O_{19}$
1-nitro-2-nitrosobenzene	s, sub	$C_6H_4N_2O_3$	diazoaminobenzene (1,3-diphenyl-1-triazene)	s	$C_{12}H_{11}N_3$
1-nitro-3-nitrosobenzene	s, sub	$C_6H_4N_2O_3$	5,7-dinitro-1-picrylbenzotrizole	s	$C_{12}H_4N_8O_{10}$
1,2-dinitrobenzene	s	$C_6H_4N_2O_4$			

[a] Molecules in italics did not have an experimental crystal structure that could be used as a starting structure in the geometry optimizations. [b] Symbols denote what type of experimental data are available for each species: gas-phase heat of formation (g), liquid-phase heat of formation (l), solid-phase heat of formation (s), heat of sublimation (sub), and heat of vaporization (v). [c] References 21, 22. [d] References 25. [e] Molecules were not included in statistical analyses due to large errors or questionable experimental data. [f] Reference 26.

3). The latter two descriptors reflect shape and connectivity characteristics. PNSA (partial negative surface area), PPSA (partial positive surface area), and RNCG (relative negative charge) are electrostatic descriptors, while TMSA is an acronym for total molecular surface area. Since the EPS method has demonstrated a correlation between the heats of vaporization or sublimation and statistically based quantities associated with the ESP on an isosurface of electron density, it is not surprising that the optimum set of QSPR descriptors contains those associated with electrostatics.

4. Results and Discussion

4.1. Results of the Fitting. Atom and group equivalents using either the 6-31G* or 6-311++G(2df,2p) energies were obtained by fitting eq 1 to the experimental values of $\Delta H°_{f(g)}$ for all molecules in the training set, and the results for the 6-311++G-(2df,2p) basis set are given in Table 3. Table 4 gives the rms and maximum deviation of $\Delta H°_{f(g)}$ values calculated using eq 1 and these atom or group equivalents from the experimental values in the training set. The rms deviation is decreased when using group versus atom equivalents for both basis sets, with the largest improvement for the 6-31G* basis set. There is also noticeable improvement in moving from the smaller to the larger

TABLE 3: Atom or Group Equivalent Energies and Parameters for Eqs 3 and 4 Using B3LYP/6-31G* Geometries, B3LYP/6-311++G(2df,2p) Energies, and Electrostatic Surface Potential Mappings

atom or group equivalent	ϵ (hartree)	eq 3		eq 4	
C	−38.123 748	a^a	2.130 167	a^b	0.000 267
H	−0.597 580	b^c	0.930 065	b^c	1.650 087
N	−54.785 466	c^c	−17.843 973	c^c	2.966 078
O	−75.187 087				
C′	−38.129 456				
N′	−54.788 487				
O′	−75.186 033				
C−NO_2	−205.160 396				
C′−NO_2	−205.163 484				
N−NO_2	−205.166 631				
O−NO_2	−164.364 907				
C−N_3	−129.976 691				

[a] In kcal/mol-Å^{-1}. [b] In kcal/mol-Å^{-4}. [c] In kcal/mol.

TABLE 4: Root Mean Square and Maximum Deviation Errors (kcal/mol) for the Gas-Phase Heats of Formation Using Either the 6-31G* or 6-311++G(2df,2p) Energies and Atom or Group Equivalents[a]

	6-31G* energy		6-311++G(2df,2p) energy	
	atom equivalent	group equivalent	atom equivalent	group equivalent
rms	3.9	3.1	3.0	2.9
max dev	8.8	10.3	8.3	9.1

[a] Structures are optimized at the B3LYP/6-31G* level.

basis set. The procedure that shows the greatest improvement over that given in Rice et al.[10] uses group equivalents and the larger basis set; results are given in Table 1S. For this method, the rms error is 2.9 kcal/mol. Parameters obtained by fitting eqs 3 and 4 to the training set of experimental values and B3LYP/6-311++G(2df,2p)//6-31G* electrostatic surface potential mappings are also presented in Table 3. Calculated ΔH_{sub} and ΔH_{vap} using these parameters are given in Table 1S. The rms deviations of the ΔH_{sub} and ΔH_{vap} from experiment are 3.1 and 2.1 kcal/mol, respectively, similar to that reported in Rice et al.[10] The maximum deviation of the ΔH_{sub} and ΔH_{vap} from experiment are 7.0 and 4.5 kcal/mol, respectively, somewhat better than that reported in Rice et al.[10] These values and the large basis set, group equivalent gas phase heats of formation were used in eq 2 to produce condensed phase heats of formation for training set molecules (also given in Table 1S). The rms deviations for the liquid and solid phase heats of formation are 3.3 and 4.9 kcal/mol, respectively. The rms errors in the condensed phase heats of formation are larger than either of the components used to evaluate them [eq 2], which is not surprising since the error is additive. In an attempt to reduce some of the error in the solid phase heat of formation that might be due to error in the heats of sublimation, we calculated solid phase heats of formation using QSPR predictions of the heat of sublimation as described in section 3.

Predictions using the five-descriptor QSPR fitted to all but four of the training set molecules produce rms and maximum errors of 0.8 and 1.7 kcal/mol, respectively, in the heats of sublimation, substantially smaller than those calculated for the same subset of training molecules using the ESP method (3.1 and 7.0 kcal/mol, respectively). The four molecules HNS [(1,1′-(1,2-ethenediyl)bis[2,4,6−trinitrobenzene], *N*-nitrobis-2,2,2-trinitroethylamine, trityl azide and *N*-nitrobis-2,2-dinitropropylamine] were not included in this exercise because the QSPR description of the heat of sublimation requires information obtained in a thermochemistry analysis (as implemented in the Gaussian03 program package) of information generated in the DFT calculations. Such an analysis can be obtained only after evaluating the second derivatives of the energy with respect to the Cartesian nuclear coordinates. As indicated in section 3, normal-mode analyses were not conducted for molecules with more than 21 heavy atoms due to the computational expense associated with these calculations. The application of QSPR predictions of the heat of sublimation along with the large basis set group equivalent gas phase heats of formation in eq 2 produces solid phase heats of formation that are in better agreement with experiment than those calculated using the ESP method. The QSPR $\Delta H°_{f(s)}$ values have rms and maximum deviations of 3.6 and 9.6 kcal/mol from experiment for this subset of training molecules, while results generated using the ESP method have rms and maximum deviations of 4.1 and 10.6 kcal/mol, respectively, for the same subset.

4.2. Predictive Capability. Because these computational methodologies are being developed to aid in the evaluation of potential performance of materials that have not yet been synthesized, it is crucial that their predictive capability be assessed, and the degree of error determined, if possible. Toward these goals, we have calculated the thermodynamic values for each molecule in the test set. These results can be considered as truly predicted, since no information about these molecules was used in determining the parameters for eqs 1, 3, and 4. The calculated thermodynamic values for all molecules in the test set using the group equivalents and the 6-311++G(2df,2p) basis set are provided for comparison with available experimental information in Table 1S.

TABLE 5: Root Mean Square Deviation and Maximum Deviation Errors (kcal/mol) of Heats of Formation and Phase Change for Molecules That Were Not Used in the Parametrization of the Methods

		current study			
		atom equivalent[b]		group equivalent[b]	
	no. of molecules[a]	rms error	max error	rms error	max error
$\Delta H°_{f(g)}$	15	2.8	5.4	3.2	6.5
$\Delta H°_{f(l)}$	24	3.1	7.2	3.2	7.4
$\Delta H°_{f(s)}$	49	6.0	16.7	5.6	12.2
ΔH_{vap} [c]	20	3.0	6.3	3.0	6.3
ΔH_{sub} [c]	6	4.7	6.8	4.7	6.8

[a] This column contains the number of molecules for which there were experimental data available for comparison. [b] 6-311++G(2df,2p) energies. [c] Atom or group equivalents are not used in evaluation.

Rms and maximum errors for completely predicted heats of formation and heats of vaporization and sublimation using the large basis set energies were calculated for all but five molecules in the test suite, and are reported in Table 5. Three molecules in the test suite were eliminated in our statistical analyses due to predictions of $\Delta H°_{f(s)}$ that are lower than experiment by at least 38 kcal/mol, an order of magnitude larger than the rms error. These molecules are 5,5′-hydrazotetrazole, DPT (dinitropentamethylene-tetramine), and 1-nitro-3-guanidinourea. The 5,5-hydrazotetrazole molecule is composed of a pair of tetrazole rings bound by a nitrogen pair. As the only molecule in this study that has a high nitrogen content, it is not surprising that the descriptions of correlations in this study are unable to account for this compound. 1-Nitro-3-guanidinourea has a double bonded NH group, another chemical species that has not been included in the training set of molecules. DPT is a bridged compound with nitrogen as the links to the carbon bridge, and thus not well represented by species contained in the training suite. Therefore, these clearly demonstrate that the computational tool is limited to chemical systems that are similar to those used in the parametrization of eqs 1, 3, and 4 and should not be applied with confidence to dissimilar chemical systems. The remaining two molecules that were removed from the statistical analyses were eliminated because the experimentally derived ΔH_{vap} values were determined from surface tension measurements through an empirically based equation and were considered by the experimentalists as "approximate".[36] The corresponding $\Delta H_{f(l)}$ values for the azidocyclopentane and azidocyclohexane molecules are smaller than the experimental value using either the atom or group equivalent methods by ~7 and ~12.5 kcal/mol, respectively. For the remaining molecules in the test set, the predicted gas and liquid phase heats of formation calculated using the method of atom equivalents are in better agreement with experiment than those calculated using the method of group equivalents. However, the rms error in the predicted solid phase heats of formation is better using the method of group equivalents.

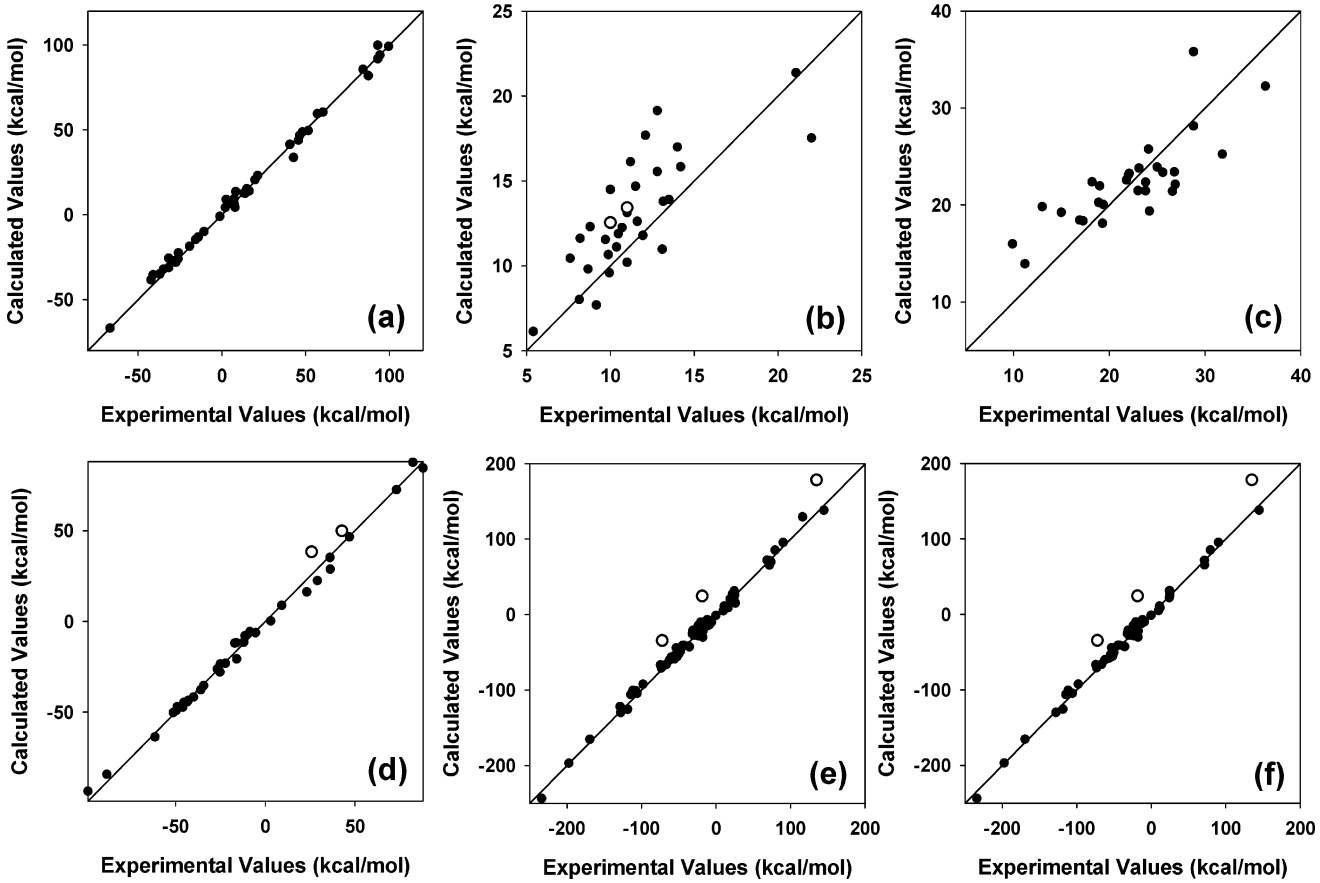

Figure 1. Calculated thermodynamic values versus experimental data for all molecules in the test and training sets: (a) gas phase heat of formation; (b) heat of vaporization; (c) heat of sublimation; (d) liquid phase heat of formation; (e) solid phase heat of formation; and (f) solid phase heat of formation for test set molecules only. The five molecules that are not included in the statistical analyses (see text) are represented as open circles in panels b, d, e, and f. The solid line bisecting each figure along the diagonal represents exact agreement between the calculated and experimental values.

Figure 1a−e provides a visual comparison between experimental and calculated values for the heats of formation, heats of sublimation, and heats of vaporization for all systems contained in both training and test sets (Tables 1 and 2). Figure 1f provides a comparison between calculated and experimental values of the solid phase heats of formation for the test suite molecules only. In each of these figures, exact agreement between the experimental and theoretical values is represented by the line that bisects each figure along the diagonal. With the exception of the heat of vaporization [Figure 1b], the points are distributed approximately equally on either side of this line. In Figure 1b, however, the distribution of points indicates that the calculated heats of vaporization are, for the most part, larger than the experimental values. Six of the points in this figure can be traced to poor predictions of azido compounds, in particular, the azido-chain aliphatic molecules in the test set (1-azidopentane, 1-azidohexane, 1-azidoheptane, and 1-azidooctane). The predicted heats of vaporization for these molecules are higher than the experimental values by 4.5 to 6.3 kcal/mol, with the error increasing with increasing size of aliphatic chain. Unfortunately, very few azido compounds were included in our training set of molecules although the azido functionality is beginning to be more prevalent in candidate advanced energetic materials. The training set contains seven azido compounds, and only four of these have experimental values for the heats of sublimation. Two of these have multiple nitro functional groups within their structure, and the remaining two have benzene rings. Conversely, there are six azido compounds in the test set; four are the azido chain aliphatic compounds with no other functional groups in the molecular structure. The remaining two are the azido cyclic compounds that were described earlier as having unreliable experimental values. The differences between experimental and predicted values for heats of sublimation for the azido cyclic compounds are 2.4 and 2.5 kcal/mol.

As was done for a subset of training suite molecules, we applied the QSPR method of predicting heats of sublimation to a subset of test suite molecules to determine if predictions of the solid phase heats of formation would improve. The subset consists of all test suite molecules with no more than 21 heavy atoms. Additionally, we did not include the three test suite molecules that were eliminated in our statistical analyses due to extremely poor predictions of $\Delta H°_{f(s)}$ using the ESP method, as described earlier. Predicted heats of sublimation using the QSPR method for this subset of molecules produced an rms error of 5.2 kcal/mol with a maximum error of 8.9 kcal/mol, compared to 4.7 and 6.8 kcal/mol for the same subset of training set molecules using the ESP method. Predictions of the solid phase heats of formation using the QSPR method also have poorer agreement with experiment than results calculated using the ESP method. The rms error in the solid phase heats of formation using the five descriptor QSPR fit and the group additivity gas phase heat of formation is 6.4 kcal/mol compared to 5.5 kcal/mol using the ESP method. Similarly, the maximum error using the QSPR method is 20.9 kcal/mol, compared to 12.2 kcal/mol for the ESP method.

We also attempted a five descriptor fit to the available heats of sublimation data for molecules with no more than 21 heavy atoms contained within both training and test sets and achieved

TABLE 6: Root Mean Square Deviation (kcal/mol) for Heats of Formation for Gas-, Liquid-, and Solid-Phase and Heats of Phase Change for Series of Molecules Common to the Rice et al. Study[a] and the Current Investigation

			current study	
	original Rice et al. results[a]	reanalyzed Rice et al. results	group equiv, B3LYP/6-311++G(2df, 2p)//B3LYP/6-31G* energy	group equiv, MP2/6-31G*// B3LYP/6-31G* energy
$\Delta H°_{f(g)}$	3.1 (7.3)	3.0 (7.3)	3.0 (9.1)	4.3 (10.0)
$\Delta H°_{f(l)}$	3.3 (9.3)	3.4 (9.3)	2.5 (5.0)	4.7 (12.4)
$\Delta H°_{f(s)}$	9.0 (35.4)	8.6 (25.7)	4.7 (12.2)	6.7 (21.8)
ΔH_{vap}	1.7 (6.1)	1.9 (6.1)	2.1 (4.5)	2.5 (4.8)
ΔH_{sub}	3.6 (12.4)	3.1 (6.0)	3.5 (6.8)	3.4 (7.5)

[a] Reference 10. [b] Maximum deviation is given in parentheses.

a 1.7 kcal/mol rms error versus experiment for the ΔH_{sub}. However, the application of this QSPR ΔH_{sub} tool to generate heats of sublimation for the prediction of $\Delta H°_{f(s)}$ produces a rms error of 6.4 kcal/mol in the solid phase heats of formation, the same as that using the five-descriptor fit to the training suite of data. Because the QSPR method reflects an approximately a 1 kcal/mol drop in accuracy compared to the ESP method, we see no benefit to using the alternate QSPR method to predict the heats of sublimation for use in prediction of solid phase heats of formation.

An inspection of the experimental data revealed inconsistencies in the reported information. After analyzing the 17 molecules in the test set for which there are ΔH_{sub}, $\Delta H°_{f(g)}$, and $\Delta H°_{f(s)}$ data, we calculated $\Delta H°_{f(s)}$ using eq 2 and the experimental values of ΔH_{sub} and $\Delta H°_{f(g)}$. We then compared the resulting values with the reported experimental solid phase heats of formation. Three molecules exhibited significant differences in the solid phase heats of formation: DMNO (6.8 kcal/mol), TNT (−4.2 kcal/mol), and TTT (−0.9 kcal/mol). The remaining molecules had differences under 0.3 kcal/mol. Our rms error of approximately 4.5 kcal/mol in the solid phase heats of formation approaches the differences seen in the experimental results, at least for these three molecules.

4.3. Comparison with Rice et al. A direct comparison of the results of this study to those of Rice et al.[10] is necessary to determine if a newer set of predictive capabilities is to be used in calculating thermodynamic information of CHNO systems. Thus, we wish to comment on and subtly alter the statistics from the previous work in order to achieve such a comparison. Before a comparison can be accomplished, the disparity in the sample molecules used in the previous and the current works must be addressed. Additionally, when parametrizing the atom equivalents and heats of phase change equations, Rice et al.[10] included systems that had multiple different experimental values, thus adding some bias into the fitting. In addressing the latter issue, we have taken the predicted results from Rice et al. and recomputed the rms and maximum error for the various heats of formation and the heats of vaporization and sublimation using the same paradigm as employed in the current work, i.e., using only the most recent experimental data for comparison. The ensuing changes are minor (shown in Table 6); however, we considered this necessary in order to avoid confusion in contrasting the current findings with the previous results.

The Rice et al. and the large basis set group equivalent results of the rms and maximum errors for the heats of formation and phase change for a set of 42 molecules common to both studies are given in Table 6. This common set of molecules includes species whose thermodynamic information was completely predicted and some that were used in parametrizing eqs 1, 3, and 4. While there is minimal change in the $\Delta H°_{f(g)}$, there is noticeable difference in the $\Delta H°_{f(l)}$ and $\Delta H°_{f(s)}$ over the same data set, with a 45% improvement in the rms error for the solid phase heat of formation when using the large basis set group equivalent scheme presented in this paper. For the ΔH_{vap} and ΔH_{sub}, the rms errors are lower for the previous results, although the difference is smaller for the ΔH_{vap} over the same range of data.

In comparing the predictive capability of the Rice et al. method[10] and that presented here, we identified 16 molecules in our test set that were not used in the parametrization of equations in the Rice et al. study. For this set of 16 molecules, the rms deviation of $\Delta H°_{f(s)}$ with experiment using the Rice et al. method is 7.1 kcal/mol, whereas the rms of $\Delta H°_{f(s)}$ from experiment calculated using the atom equivalent B3LYP/6-311++G(2df,2p) parameters is 6.1 kcal/mol, a 1 kcal/mol improvement in going to the larger basis set. An additional ∼0.3 kcal/mol improvement is attained upon application of the group equivalent scheme; the resulting rms deviation of $\Delta H°_{f(s)}$ from experiment is 5.7 kcal/mol. Also, the predicted maximum deviation using the group equivalent scheme (12.2 kcal/mol) is more than 5 kcal/mol smaller than that reported by Rice et al. (17.3 kcal/mol). Therefore, for the same predictive data set, the large basis group additivity method demonstrates significant improvement over the previous work for the solid state heats of formation.

Turning to a closer inspection of the outliers for each thermodynamic value, we first examine the gas phase heats of formation. For both the atom and group equivalent methods using the large basis set, hexanitroethane was underpredicted by 8.3 and 9.1 kcal/mol, respectively, even though it was included in the fitting set. In comparison, Rice et al. exhibited a 1.1 kcal/mol overprediction for this molecule; this system was also included in their fitting set. The largest error in the predicted set of molecules for the group equivalent scheme was 9.1 kcal/mol for the 3,4-furazandimethanol dinitrate molecule, which displayed a −6.5 kcal/mol error in ref 10. In the previous work, however, information about this molecule was used in the parametrization of eqs 1 and 3. Also, in the previous work the largest error for gas phase heats of formation was 7.3 kcal/mol for azidomethylbenzene, which we predict with an error of 0.4 kcal/mol.

For the liquid phase heats of formation, the largest error in the current study is 7.4 kcal/mol for 1-azidohexane. In the previous work, azidomethylbenzene displayed a maximum error of 9.3 kcal/mol, versus a current prediction of 3.5 kcal/mol. For both the current and previous studies, 2,4,6-trinitroresorcinol presented a troublesome prediction for the solid phase heats of formation, with errors of −11.1 and −17.3 kcal/mol, respectively. The largest error seen in the current work is 13.3 kcal/mol for trityl azide, which was not included in the previous study. The largest error in $\Delta H°_{f(s)}$ reported in the Rice et al. study was 25.7 kcal/mol for HNS; the value produced using the group equivalent method and larger basis set has a 7.3 kcal/mol error when compared to experiment.

Looking to the heats of vaporization, the maximum error reported in this study is −6.3 kcal/mol for 1-azidooctane. The maximum error for this value in the Rice et al. study was for nitroglycerin, which was underpredicted by 6.1 kcal/mol, while the current study has an error of 4.5 kcal/mol. The largest error for the heats of sublimation in this study is for trityl azide, with a −7.0 kcal/mol error. In the previous study,[10] the maximum error was 6.0 kcal/mol for 1,4-dintrosopiperazine, while the

current ESP method of evaluating heats of sublimation produces a 4.9 kcal/mol error.

4.4. Comparison with a Non-DFT Method. A critical component to the success of this method is for a molecule's electrostatic potential to exhibit a correlation with the bulk property of interest, in this case the heat of vaporization or sublimation. Thus, it is also important to analyze the dependence of the results with other non-DFT ab initio theories. The purpose of this section is to ascertain the effect of explicit correlation on the molecular electrostatic potential, and effects on the predictive capabilities. Therefore, we will compare thermodynamic properties as predicted using DFT to those generated using non-DFT results.

For the purposes of this comparison, we will use second-order Møller−Plesset perturbation theory (MP2).[37] MP2 is a commonly used, lower-order correlated method due to its relatively modest computational requirements compared to more correlated theories. However, MP2 calculations require more computational resources than DFT methods. Therefore we first established the size of the basis set we could use for the molecules in Table 6 when applying the MP2 method. The largest molecule in this set is HNS (1,1′-(1,2-ethenediyl)bis-[2,4,6-trinitrobenzene]). Attempts to generate single point calculations at the MP2/6-311++G(2df,2p)//B3LYP/6-31G* level were unsuccessful due to memory requirements, even when attempted on DoD High Performance Computing Multi-Shared Resource Center platforms. As this tool was meant to be used by those without supercomputer resources, we deemed that using MP2/6-311++G(2df,2p) would not be feasible for most researchers, and thus, not useful for the purposes of the development of the tool.

We performed a series of MP2/6-31G*//B3LYP/6-31G* calculations over the molecules listed in Table 6. The results of that series of calculations are given in Table 6. As is evident, the MP2/6-31G* solid phase heats of formation are only better than the original and reanalyzed Rice et al. values, not the B3LYP/6-311++G(2df,2p) results. The MP2/6-31G* gas and liquid phase heats of formation are worse than all DFT-based values. Thus, it is apparent that MP2 is not computationally viable using the 6-311++G(2df,2p) basis set, and the MP2/6-31G* method does not improve upon the B3LYP/6-311++G-(2df,2p) predictions.

5. Summary and Conclusions

We have modified the work of Rice et al.[10] in the prediction of gas, liquid, and solid heats of formation, heat of vaporization, and heat of sublimation using quantum mechanical data through the incorporation of group additivity and the use of the 6-311++G(2df,2p) basis set. The resulting equations used to predict heats of formation or phase change are applied to molecules for which no information was used in the parametrization of the tools. The rms deviation of the predicted gas phase heats of formation from experiment is 3.2 kcal/mol with a maximum deviation of 6.5 kcal/mol. The rms deviations in the heats of vaporization and sublimation are 3.0 and 4.7 kcal/mol, respectively; corresponding maximum deviations are 6.3 and 6.8 kcal/mol, respectively. The rms and maximum deviation of the predicted liquid phase heats of formation are 3.2 and 7.4 kcal/mol, respectively. Finally, the rms and maximum deviation of predicted solid phase heats of formation are 5.6 and 12.2 kcal/mol, respectively, a significant improvement (>40%) in the rms deviation relative to results using an earlier method proposed by Rice et al.[10] We also calculated solid phase heats of formation using heats of sublimation predicted using QSPR methods, and compared these with results generated using the ESP method. The comparison shows that the ESP method is more accurate than the QSPR method in calculating solid phase heats of formation, indicating no benefit in using the alternate QSPR approach.

Acknowledgment. All calculations were performed at the Army Research Laboratory Major Shared Resource Center, an initiative of the DOD High Performance Computing Modernization Program. This work was supported in part by the Research Development and Engineering Command Ordnance Environmental Program to address Environmental Quality Technology Requirements.

Supporting Information Available: Table of heats of formation, vaporization, and sublimation (Table 1S) and table of molecular properties used in eqs 1, 3, and 4 (Table 2S). This material is available free of charge via the Internet at http://pubs.acs.org.

References and Notes

(1) Rice, B. M. In *Overviews of Recent Research in Energetic Materials*; Thompson, D. L., Brill, T. B., Shaw, R. W., Eds.; World Scientific of Singapore: London, Hong Kong, Dover, New Jersey, 2003.

(2) Mathieu, D.; Simonetti, P. *Thermochim. Acta* **2002**, *384*, 369.

(3) Politzer, P.; Murray, J. S.; Seminario, J. M.; Lane, P.; Grice, M. E.; Concha M. C. *J. Mol. Struct. (THEOCHEM)* **2001**, *573*. Politzer, P.; Murray, J. S. *Fluid Phase Equilib.* **2001**, *185*, 129.

(4) Politzer, P.; Murray, J. S.; Grice, M. E.; DeSalvo, M.; Miller, E. *Mol. Phys.* **1997**, *91*, 923.

(5) Murray, J. S.; Politzer, P. *J. Mol. Struct. (THEOCHEM)* **1998**, *425*, 107.

(6) Kim, C. K.; Lee, K. A.; Hyun, K. H.; Park, H. J.; Kwack, I. Y.; Kim, C. K.; Lee, H. W.; Lee, B. S. *J. Comput. Chem.* **2004**, *25*, 2073.

(7) Politzer, P.; Lane, P.; Concha, M. C. *Struct. Chem.* **2004**, *15*, 469.

(8) Mathieu, D.; Simonetti, P. *Thermochim. Acta* **2002**, *384*, 369.

(9) Politzer, P.; Lane, P.; Concha, M. C. In *Energetic Materials Part 1. Decomposition, Crystal and Molecular Properties*; Politzer, P. P., Murray, J. S., Eds.; Elsevier: Amsterdam, 2003; p 247.

(10) Rice, B. M.; Pai, S. V.; Hare, J. *Combust. Flame* **1999**, *118*, 445.

(11) Curtiss, L. A.; Raghavachari, K.; Redfern, P. C.; Rassolov, P. C.; Pople, J. A. *J. Chem. Phys.* **1998**, *109*, 7764.

(12) Curtiss, L. A.; Raghavachari, K.; Redfern, P. C.; Pople, J. A. *J. Chem. Phys.* **1997**, *106*, 1063.

(13) Melius, C. F. In *Chemistry and Physics of Energetic Materials*; Bulusu, S. N., Ed.; Kluwer Academic Publishers: Dordrecht, 1990; Vol. 309, p 21.

(14) Atkins, P. W. *Physical Chemistry*; Oxford University Press: Oxford, 1982.

(15) Hohenberg, P.; Kohn, W. *Phys. Rev. B* **1964**, *136*, 864.

(16) Kohn, W.; Sham, L. J. *Phys. Rev. A* **1965**, *10*, 113.

(17) Politzer, P.; Murray, J. S.; Brinck, T.; Lane, P. In *Immunoanalysis of Agrochemicals*; Nelson, J. O., Karu, A. E., Wong, R. B., Eds.; ACS Symp. Ser. 586; American Chemical Society: Washington, DC, 1994; Chapter 8.

(18) Murray, J. S.; Politzer, P. Quantitative Treatment of Solute/Solvent Interactions. In *Theoretical and Computational Chemistry*; Politzer, P., Murray, J. S., Eds.; Elsevier Scientific: Amsterdam, 1994; 1, pp 243−289.

(19) Politzer, P.; Murray, J. S. *J. Phys. Chem. A* **1998**, *102*, 1018.

(20) Vladimiroff, T. U.S. Army Armament Research, Development and Engineering Center, Picatinny Arsenal, NJ, private communication.

(21) Unless otherwise noted, all experimental thermodynamic values reported in this work were obtained from the NIST Standard Reference Database Number 69, which can be accessed electronically through the NIST Chemistry Web Book (URL http://webbook.nist.gov/chemistry/); references are given therein.

(22) All structural information is obtained from the Cambridge Structural Database (CSD). Allen, F. H. *Acta Crystallogr.* **2002**, *B58*, 380.

(23) Pepkin, V. I.; Matyushin, Yu. N.; Khisamutdinov, G. Kh.; Slovetskiy. V. I.; Fayzil'berg, A. A. *Khim. Fiz.* **1993**, *12*, 1399.

(24) Wayne, G. H. S.; Synder, G. J. *J. Am. Chem. Soc.* **1993**, *115*, 9860.

(25) Ostmark, H.; Langlet, A.; Bergman, H.; Wingborg, N.; Wellmar, U.; Beem, U. "Fox-7−A New Explosive with Low Sensitivity and High Performance" FOA, Defense Research Establishment, SE-172 90 Stockholm, Sweden.

(26) Simpson, R. L.; Urtiew, P. A.; Ornellas, D. L.; Moody, G. L.; Scribner, K. J.; Hoffman, D. M. *Propellants, Explos., Pyrotech.* **1997**, *22*, 249.

(27) Becke, A. D. *J. Chem. Phys.* **1993**, *98*, 5648.

(28) Lee, C.; Yang, W.; Parr, R. G. *Phys. Rev.* **1988**, *B41*, 785.

(29) Hariharan, P. C.; Pople, J. A. *Theor. Chim. Acta* **1973**, *28*, 213.

(30) Frisch, M. J.; Trucks, G. W.; Schlegel, H. B.; Scuseria, G. E.; Robb, M. A.; Cheeseman, J. R.; Montgomery, J. A., Jr.; Vreven, T.; Kudin, K. N.; Burant, J. C.; Millam, J. M.; Iyengar, S. S.; Tomasi, J.; Barone, V.; Mennucci, B.; Cossi, M.; Scalmani, G.; Rega, N.; Petersson, G. A.; Nakatsuji, H.; Hada, M.; Ehara, M.; Toyota, K.; Fukuda, R.; Hasegawa, J.; Ishida, M.; Nakajima, T.; Honda, Y.; Kitao, O.; Nakai, H.; Klene, M.; Li, X.; Knox, J. E.; Hratchian, H. P.; Cross, J. B.; Adamo, C.; Jaramillo, J.; Gomperts, R.; Stratmann, R. E.; Yazyev, O.; Austin, A. J.; Cammi, R.; Pomelli, C.; Ochterski, J. W.; Ayala, P. Y.; Morokuma, K.; Voth, G. A.; Salvador, P.; Dannenberg, J. J.; Zakrzewski, V. G.; Dapprich, S.; Daniels, A. D.; Strain, M. C.; Farkas, O.; Malick, D. K.; Rabuck, A. D.; Raghavachari, K.; Foresman, J. B.; Ortiz, J. V.; Cui, Q.; Baboul, A. G.; Clifford, S.; Cioslowski, J.; Stefanov, B. B.; Liu, G.; Liashenko, A.; Piskorz, P.; Komaromi, I.; Martin, R. L.; Fox, D. J.; Keith, T.; Al-Laham, M. A.; Peng, C. Y.; Nanayakkara, A.; Challacombe, M.; Gill, P. M. W.; Johnson, B.; Chen, W.; Wong, M. W.; Gonzalez, C.; Pople, J. A. *Gaussian 03*, revision A.1; Gaussian, Inc.: Pittsburgh, PA, 2003.

(31) McLean, A. D.; Chandler, G. S. *J. Chem. Phys.* **1980**, *72*, 5639.

(32) Krishnan, R.; Binkley, J. S.; Seeger, R.; Pople, J. A. *J. Chem. Phys.* **1980**, *72*, 650.

(33) Karelson, M. *Molecular Descriptors in QSAR/QSPR*; John Wiley and Sons: New York, 2000.

(34) Katritzky, A. R.; Lobanov, V. S.; Karelson, M. *Chem. Soc. Rev.* **1995**, 279.

(35) CODESSA is a quantitative structure/activity relationship (QSAR) program and is the result of a joint effort between Semichem, Inc., and Professors Alan Katrizky (University of Florida) and Mati Karelson (University of Tartu, Estonia) (URL http://www.semichem.com/codessa/index.shtml**)**.

(36) Fagley, T. F.; Myers, H. W. *J. Am. Chem. Soc.* **1954**, *76*, 6001.

(37) Møller, C.; Plesset, M. S. *Phys. Rev.* **1934**, *46*, 618.